applied sciences

MDPI

Article

Leveraging Industrial Jarosite Waste for Arsenic(V) and Chromium(III) Adsorption from Water: A Preliminary Study

Montserrat Cruz-Hernández [1], Alondra García-Cerón [1], Ramón G. Salinas Maldonado [1], Irma A. Corro-Escorcia [1], Juan Hernández-Ávila [1], Eduardo Cerecedo-Sáenz [1], Javier Flores-Badillo [1], Norman Toro [2], Manuel Saldana [2,3], M. P. Gutiérrez-Amador [4], F. R. Barrientos-Hernández [1,*] and Eleazar Salinas-Rodríguez [1,*]

[1] Área Académica de Ciencias de la Tierra y Materiales, Instituto de Ciencias Básicas e Ingeniería, Universidad Autónoma del Estado de Hidalgo, Carretera Pachuca-Tulancingo km. 4.5, Mineral de la Reforma, Hidalgo 42184, Mexico; ing.cruzaei@hotmail.com (M.C.-H.); ga337807@uaeh.edu.mx (A.G.-C.); sa380249@uaeh.edu.mx (R.G.S.M.); coq03093@uaeh.edu.mx (I.A.C.-E.); herjuan@uaeh.edu.mx (J.H.-Á.); eduardoc@uaeh.edu.mx (E.C.-S.); javier_flores11060@uaeh.edu.mx (J.F.-B.)
[2] Facultad de Ingeniería y Arquitectura, Universidad Arturo Prat, Iquique 1100000, Chile; notoro@unap.cl (N.T.); masaldana@unap.cl (M.S.)
[3] Departamento de Ingeniería Química y Procesos de Minerales, Universidad de Antofagasta, Antofagasta 1270300, Chile
[4] Escuela Superior de Apan, Universidad Autónoma del Estado de Hidalgo, Carretera Apan-Calpulalpan, km. 8, Apan, Hidalgo 43920, Mexico; amadorg@uaeh.edu.mx
* Correspondence: profe_3193@uaeh.edu.mx (F.R.B.-H.); salinasr@uaeh.edu.mx (E.S.-R.); Tel.: +54-771-126-3933 (F.R.B.-H.); +52-771-207-4171 (E.S.-R.)

Featured Application: This preliminary research demonstrates the potential of a toxic and hazardous mining residue to adsorb As(V) and Cr(III) from contaminated waters. The next step could be the incorporation of this waste (industrial jarosite) into a porous concrete (ACC) and perhaps successfully increasing its adsorption capacity. This innovative approach offers a promising solution for the removal of toxic heavy metals from polluted water sources, providing a potential application in water treatment and remediation technologies.

Abstract: The global problem of water scarcity is exacerbated by the continued contamination of potable water sources. This preliminary study investigates the potential of a hazardous industrial jarosite waste to adsorb As(V) and Cr(III) from contaminated waters. The results showed that this mining waste effectively adsorbed both As(V) and Cr(III), demonstrating its potential as a low-cost and sustainable solution for water remediation along with the use of a hazardous waste that also contaminates. The adsorption process was optimized, and the effects of various parameters on the adsorption capacity were investigated. The findings of this study suggest that the use of toxic mining residues in porous concrete could provide a promising approach for the removal of toxic heavy metals from polluted water sources, contributing to the development of more sustainable and environmentally friendly water treatment technologies. A maximum adsorption of 90.6% of As(V) and 96.3% of Cr(III) was achieved, and it was verified that the industrial jarosite initially contained about 0.44% As, which was later leached during decomposition; again, the industrial jarosite was able to re-adsorb both As(V) and Cr(III).

Keywords: arsenic adsorption; chromium adsorption; industrial jarosite; polluted water treatment; environmental sustainability

check for updates

Academic Editors: Cristina Sousa Coutinho Calheiros and Ana Maria Antão Geraldes

Received: 17 December 2024
Revised: 10 January 2025
Accepted: 15 January 2025
Published: 31 January 2025

Citation: Cruz-Hernández, M.; García-Cerón, A.; Maldonado, R.G.S.; Corro-Escorcia, I.A.; Hernández-Ávila, J.; Cerecedo-Sáenz, E.; Flores-Badillo, J.; Toro, N.; Saldana, M.; Gutiérrez-Amador, M.P.; et al. Leveraging Industrial Jarosite Waste for Arsenic(V) and Chromium(III) Adsorption from Water: A Preliminary Study. *Appl. Sci.* **2025**, *15*, 1469. https://doi.org/10.3390/app15031469

Copyright: © 2025 by the authors. Licensee MDPI, Basel, Switzerland. This article is an open access article distributed under the terms and conditions of the Creative Commons Attribution (CC BY) license (https://creativecommons.org/licenses/by/4.0/).

1. Introduction

The global shortage of potable water is a pressing issue, impacting a substantial segment of the world's population, not only in food supply chains or their industrial activities but directly on global health and economy [1]. Human activities, including mining, agriculture, industrial processes, climate change, population growth, and detrimental societal practices, further aggravate this problem through water pollution [2–5].

Water pollution arises from diverse substances, including physical contaminants like sediments, suspended particles, and abnormal temperature fluctuations. Additionally, biological, radiological, petroleum-based, and chemical contaminants, such as pesticides, solvents, fertilizers, pharmaceutical waste, and heavy metals, contribute to water pollution. Many of these pollutants reach the water through industrial pipes; drainage systems in communities, towns, and large cities; and through poor disposal habits for liquid, solid or gaseous waste. There is also contamination from leaks, poor care in pesticide and fertilizer application protocols, and activities on ships and in industry, especially mining, which has little control over its operations. In general, water pollution seriously affects vital organs of the human body and the nervous system and causes various types of cancer, cardiovascular diseases, among other conditions [6–9].

Among all the pollutants mentioned above, arsenic and chromium pose significant risks, causing irreversible harm to human health and the environment. Chromium exposure is linked to cancer and neurological damage, whereas arsenic increases the risk of cardiovascular disease, kidney problems, and cancer. The presence of these metals in potable water can have catastrophic consequences, particularly for vulnerable communities reliant on contaminated water sources, due to the lack of attention to the way in which various industrial activities and public and private drainage are carried out [10,11].

Therefore, it is essential to implement measures to protect and conserve water resources, reduce pollution, and ensure access to safe and healthy water. Currently, removing arsenic and chromium from contaminated water involves various methods based on biological, chemical, and physical techniques. Among the biological methods, phytoremediation uses plants to absorb water contaminants, while bioremediation employs microorganisms to degrade pollutants [12–15]. Also, the production of biochar through the conversion of plant biomass could be a viable option for As adsorption. However, this process is typically carried out at elevated temperatures [16,17].

Alternatively, chemical methods, including precipitation, involve introducing chemical reagents to form insoluble compounds with arsenic and chromium ions, which are subsequently removed through sedimentation [18]. In some cases, combustible coal may have arsenic content that is released during such combustion, and leaching studies with ferric chloride have been carried out to remove such As content, which show the clear affinity of Fe for As [19]. On the other hand, removal of Cr(VI) was possible with the synthesis of a compound that combines NiFeMn-layered double hydroxide and Ti3C2TX MXene into gelatin via a cross-linking reaction [20]. However, all of the above processes can be expensive, and there is no verification that the waste generated is inert. Similarly, other researchers have synthesized magnetic nanoparticles based on nickel-iron supported on graphene oxide for the removal of Cr(III) contained in water, achieving, according to the authors, the preliminary removal of 17 mg/g of Cr(III) ions dissolved in water [21]. Conversely, ion exchange utilizes resins with elements that exchange ions, effectively retaining contaminants [22,23].

Physical methods, meanwhile, rely on techniques such as reverse osmosis, employing semi-permeable membranes to eliminate contaminants, but it is necessary to consider that the applicability of this technique, the treatment performance, and its cost are necessary factors in determining the most appropriate technology for treating contaminated water [24].

Furthermore, adsorption processes are utilized, primarily involving materials like activated carbon, zeolites, clays, biogenic compounds and porous materials, which effectively retain arsenic and chromium ions [25–32]. Also, some synthetic minerals are used for the removal of heavy metals, such as schwertmannite, which is synthesized by a modified chemical oxidation process to obtain nanoparticles of this compound and which has been adequately used for the adsorption of As [33–36]. This synthesized compound again shows the affinity of Fe(III) for As, since increasing the Fe content in the synthesized material improves the adsorption of As(V). Thus, the use of iron hydroxides can improve the adsorption of As(III) and As(V), when used together with the addition of an adsorbent such as calcium contained in calcite [37], which does not seem to occur with Cr, since the presence of this element in the adsorbent apparently decreases the amount of adsorbed Cr ions [38]. On the other hand, the simultaneous removal of As(V) and Cr(VI) was possible with the use of a graphene oxide functionalized ferrohydrite. Here, the greater affinity of As for Fe than Cr is clearly noted [39].

Similarly, in nature, there are groups of related minerals that are the product of oxidative and reductive processes involving iron as the main active element in the adsorption of heavy metals. Examples of minerals that could act like adsorbents for As and Cr could be beudantite [40,41], scorodite [42,43], alunite [44–46], goethite [47,48], and jarosite [49–55], among others.

Based on the above, arsenic adsorption was achieved at room temperature with synthetic potassium jarosite, with encouraging results [14]. Therefore, this study demonstrates the possibility of using industrial jarosite, considered a toxic waste, for the adsorption of As and Cr.

This preliminary study demonstrates the potential of a harmful waste like jarosite to adsorb arsenic and chromium, offering a promising solution for the removal of these contaminants from polluted water. The innovation lies in the possibility that this residue can adsorb heavy metals, then desorb or isolate them, and repeatedly adsorb and desorb them several times, which can reduce costs and improve efficiency by using a waste already considered toxic and hazardous. While this breakthrough holds great promise, its implementation may face challenges related to its scalability, cost-effectiveness, and environmental sustainability. Nevertheless, this research paves the way for further investigations and potential applications of using a toxic waste in water remediation. In both situations, the full impact could be significant for communities affected by water pollution and for the places where these toxic wastes are produced from mining activities, and this could now be a solution to eliminate any As and Cr contained in water.

So, in this study, the hypothesis is that industrial jarosite, considered a toxic waste, can be effectively used for the repeated adsorption and desorption of arsenic and chromium in contaminated water, reducing costs and improving efficiency in water remediation. Then, to investigate the proposed hypothesis, a preliminary study was conducted in which the ability of industrial jarosite to adsorb arsenic and chromium in synthetic solutions at room temperature was evaluated.

2. Materials and Methods

2.1. Sampling of Industrial Jarosite (IJ)

For the present work, the material used was a residue from the zinc industry (IJ), and the sample was taken directly from the filter presses at the zinc plant located in the city of San Luis Potosi, SLP, Mexico. The sample was obtained by plant personnel due to access restrictions for health reasons. The sample thus obtained was then homogenized, dried at 50 °C for 2 h, and stored for subsequent characterization and experiments on the decomposition and adsorption of As(V) and Cr(III).

2.2. Adsorption of As(V) and Cr(III) in IJ

The experimentation carried out was based on previous work [14] conducted with synthetic potassium jarosite, but in this case, the focus was on the adsorption of both the As(V) and Cr(III) in IJ. Known solutions of As(V), Cr(III), and As-Cr (1454.2 ppm As and 1099.3 ppm Cr) were prepared. Subsequently, the adsorption process was carried out, and the remaining liquid was analyzed by ICP, while the solid was characterized by DRX, SEM-EDS, FTIR, and XPS. Figure 1 shows the experimental setup, which consists of 3 phases as described below.

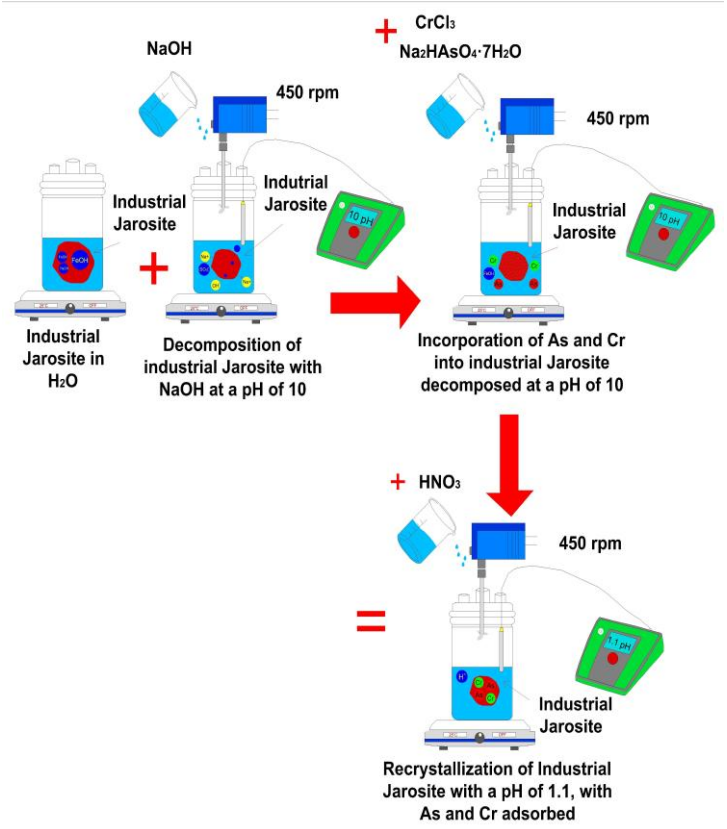

Figure 1. Experimental setup for the adsorption of As(V) and Cr(III) in the IJ and the ACC + IJ.

Firstly, to carry out the decomposition of the IJ, 3 g of material was added to 500 mL of a NaOH (Meyer brand, Mexico City, Mexico) solution until a pH of 10 was reached, which was kept constant for 10 min at room temperature. At the end of the 10 min reaction, 5 g of $Na_2HAsO_4 \cdot 7H_2O$ (Sigma-Aldrich, Burlington, MA, USA) was added, corresponding to 0.03 M. Finally, after a reaction time of 120 min, nitric acid was added to attain a pH of 1.1. After 5 min, the solution was filtered, washed, and dried for subsequent characterization to determine the amount of As(V) adsorbed. The same procedure was carried out with the addition of 3 g of IJ to a NaOH solution until a pH of 10 was attained (adding about 5–6 drops of a 1 M NaOH solution) for 10 min at room temperature. After this time, 4 g of $CrCl_3 \cdot 6H_2O$ (Meyer brand, Mexico City, Mexico) was added, which corresponds to 0.03 M. Finally, after 120 min of reaction, drops of 1M HNO_3 were added until the pH reached a value of 1.1. In a third experimental series, both reagents (As and Cr) were added simultaneously in a process like that described above.

The monitoring of As(V) and Cr(III) adsorption was carried out using Inductively Coupled Plasma Mass Spectrometry (ICP-MS). Solutions with known concentrations of As(V) and Cr(III) were prepared, and IJ samples were placed into these for 1 h with

moderate stirring. At the end, the remaining liquid was analyzed by ICP, and the percentage of As(V) and Cr(III) adsorbed in the IJ samples was determined by the difference.

2.3. Characterization of Materials

The IJ sample, the product of its alkaline decomposition, and the final product of the As(V) and Cr(III) adsorption stage (liquid and solid), were characterized using the following analytical techniques.

To disclose the mineral species contained in the samples, X-ray diffraction using the INEL Diffractometer Equinox 2000 model located at the Autonomous University of the State of Hidalgo, Mexico (AUSH) and manufactured by INEL at Artenary, Centre Val de Loire, France. For this analysis, the sweep time was 0.5 min for each sample, and the indexing for the obtained diffractograms was carried out with the MATCH version 1.1 software (developed by Crystal Impact, Bonn, Germany).

Similarly, the morphological and punctual composition analysis was performed using the JSM-IT300 JEOL Scanning Electron Microscope, manufactured by JEOL Tokyo, Japan (and located at the AUSH), using an operating voltage of 30 keV and equipped with an Oxford energy dispersive spectrometer (EDS).

In addition to determining the presence both of As(V) and Cr(III) in the resulting solids after adsorption experiments, a total reflectance Fourier-transform infrared (ATR-FTIR) analysis was carried out. This examination was performed using a Perkin Elmer Frontier FTIR spectrometer manufactured in Watham, MA, USA (and located at the AUSH), which is a high-sensitivity and high-resolution instrument capable of analyzing the infrared spectral region [56]. A 10 mg sample of powdered material was carefully placed on the crystal surface of the equipment, and each obtained spectrum was recorded as the absorbance under 75%. Each spectrum was scanned between the 4000 and 400 cm^{-1} wavelengths, covering the mid-infrared and near-infrared spectral regions [57]. FTIR spectroscopy is a widely used technique for analyzing the chemical composition of samples, providing information on the presence of functional groups and chemical bonds [58]. In this case, FTIR was used to detect the presence of As(V) and Cr(III) in the resultant solids after adsorption. The ATR-FTIR technique was employed to analyze the sample in its solid state, eliminating the need for sample preparation in a liquid or gaseous form [59].

On the other hand, the X-ray photoelectron spectroscopy (XPS) analysis was executed in a K ALPHA Surface Analysis Machine (Thermo Fisher Scientific) manufactured in Watham, MA, USA (and located at the laboratory of Nano and Biomaterials, CINVESTAV-IPN, Merida Yucatan, Mexico). This instrument has a hemispherical (180°) analyzer of double approach and a 128-channel detector with a base pressure of 2×10^{-9} mbar. The XPS spectra were first obtained in wide sweep (0–1350 V) at 1 eV/step, and then in the small-window mode at 0.1 eV/step, with a step energy of 50 eV.

Finally, the analysis performed by Inductively Coupled Plasma Mass Spectrometry (ICP-MS) was carried out with the purpose of determining the As(V) and Cr(III) contents in solution before and after conducting the adsorption experiments with the IJ samples. For this analysis, the ICP-MS equipment model 2100, manufactured by Perkin Elmer, Watham MA, USA (and located at the AUSH), was used.

3. Results and Discussion

3.1. XRD Analysis

Figure 2 shows the diffraction spectrum obtained for the IJ (A), and immediately above this spectrum, the corresponding one for the alkaline decomposed IJ (B). It can be observed that the structure of jarosite is destroyed after alkaline decomposition (second spectrum), leaving only the phase corresponding to franklinite, a phase formed during the calcination

of sphalerite and which is very stable, both to acid leaching in the zinc plant and to the alkaline decomposition carried out [60,61].

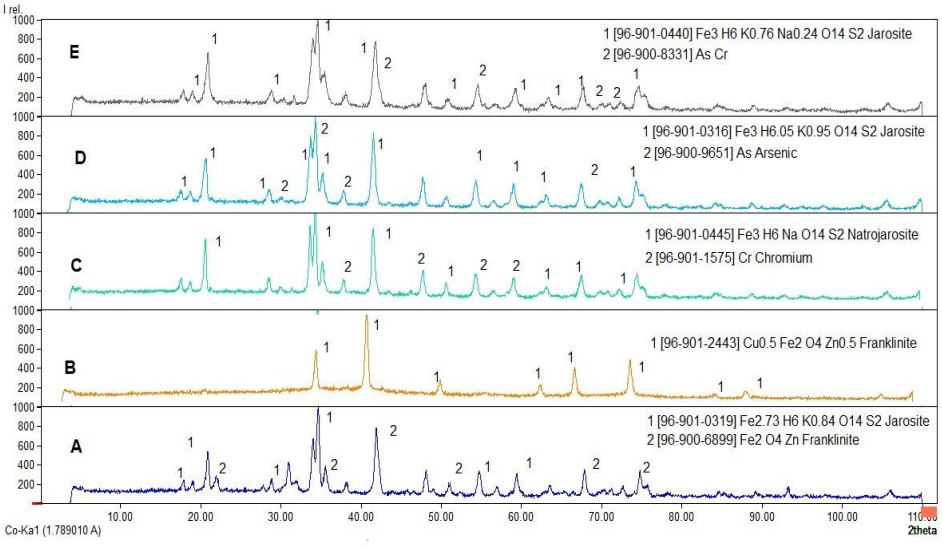

Figure 2. XRD spectra obtained for (**A**) IJ; (**B**) decomposed IJ; (**C**) IJ with As adsorbed; (**D**) IJ with Cr adsorbed; and (**E**) IJ with As-Cr adsorbed.

Also in Figure 2, above spectrum B, three additional spectra can be seen, which correspond to the solids obtained after the adsorption of Cr(III) (spectrum C), in which can be observed the presence of chromium and PDF [96-901-1575] along with the jarositic phase, which recrystallized when the pH was lowered to 1.1. On the other hand, spectrum D is that obtained after As(V) adsorption, showing the PDF [96-900-9651] that corresponds to arsenic. Finally, the last spectrum, (E), corresponds to the solids obtained after carrying out the simultaneous adsorption of As and Cr, and the corresponding PDF showing these elements is [96-900-8331]. It can be observed that in these three spectra, the jarosite phase is still present, but it is identified by different PDFs, possible due to undetermined reactions occurring during the decomposition, the adsorption process, and the recrystallization of the phase, which does not, however, alter the adsorption mechanism of these elements [14].

3.2. SEM-EDS Analysis

Figure 3 shows the images obtained by SEM, using secondary electrons (SE), of the IJ samples, decomposed IJ (IJ-D), and IJ after the adsorption of As(IJ-As), Cr (IJ-Cr), and As-Cr (IJ-As + Cr). Images were obtained at magnifications of 15,000 (left column) and 5000 (right column). A difference between IJ and IJ-D can be observed; the former shows the crystalline structure of jarosite, while in the latter, this structure has practically disappeared. The jarosite crystallizes in the hexagonal crystal system, with a crystal structure typical of the hexagonal scalenohedral type [60,61]. More specifically, jarosite has a crystal structure composed of layers of iron (Fe) octahedra and sulfate (SO_4) tetrahedra, which alternate in a hexagonal arrangement. In this type of structure, the adsorption of As on the decomposed jarosite particles, which are mainly composed of iron hydroxides ($Fe(OH)_3$), is basically due to the formation of As and Fe complexes, while the adsorption of Cr is basically due to the surface adsorption phenomena and the formation of complexes between Cr and Fe [62].

On the other hand, in the images corresponding to IJ after the adsorption of As, Cr, and As-Cr, the crystalline structure is recovered once again after undergoing decomposition, adsorption, and recrystallization processes by adjusting the pH to 1.1. This means that the waste is capable of opening its structure during decomposition, allowing the selective and simultaneous adsorption of As(V) and Cr(III) ions, and, finally, recovering its crystalline structure once these elements have been encapsulated.

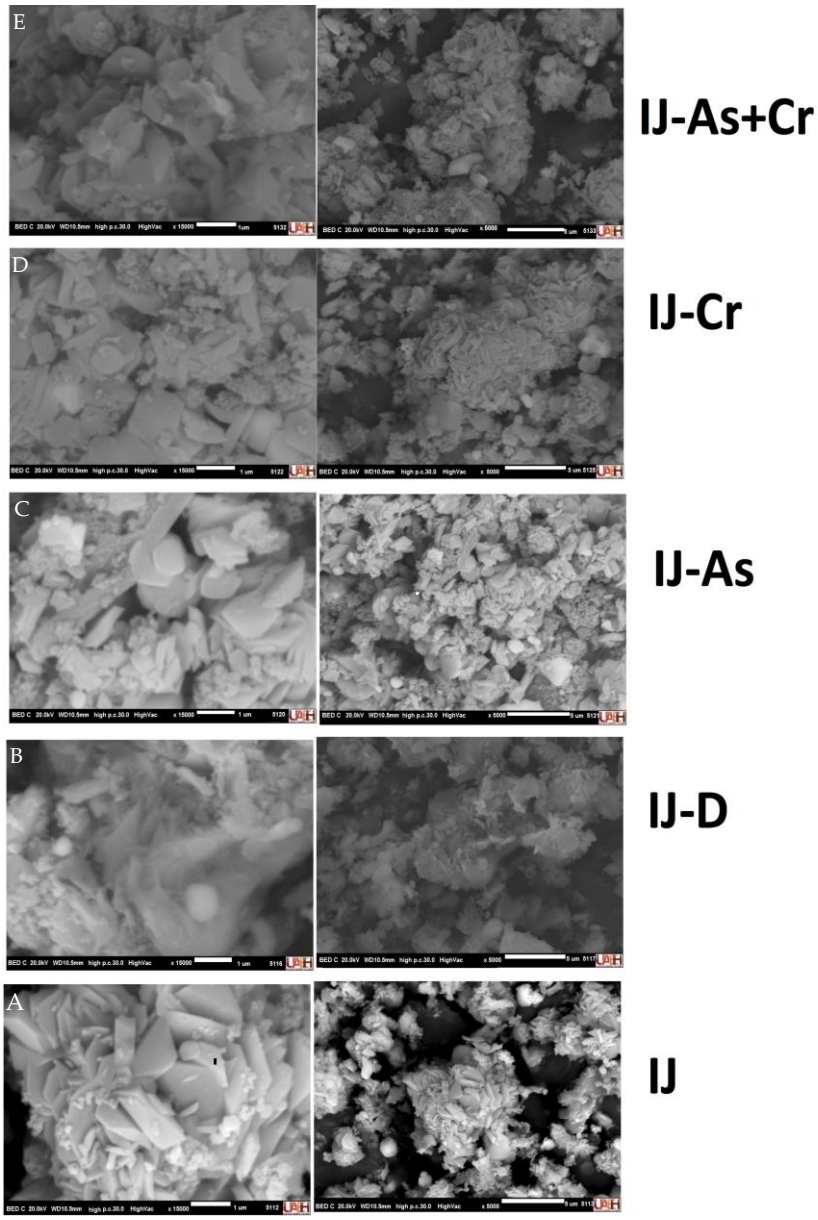

Figure 3. SEM (SE) images obtained for (**A**) IJ; (**B**) decomposed IJ; (**C**) IJ with As adsorbed; (**D**) IJ with Cr adsorbed; and (**E**) IJ with As-Cr adsorbed.

The crystallization of industrial jarosite after the adsorption of As(V) and Cr(III) ions suggests that the adsorbent material may have undergone structural and chemical changes during the adsorption process. These may be beneficial for the stabilization and immobilization of As(V) and Cr(III) ion in the matrix of the adsorbent material [14,63]. In a broader context, the results of this study have important implications for the remediation of soils and waters contaminated with As(V) and Cr(III) ions. Industrial jarosite may be a viable and cost-effective option for the adsorption of these ions compared with other more expensive adsorbent materials [27,30,31,64].

Similarly, SEM-EDS point microanalyses were performed on the various particles found using this technique. The microanalysis is point-based (approximately 1 μm^3) and semi-quantitative, and it was only performed to verify the adsorption of As(V) and Cr(III) ions on the IJ particles. However, this technique could have some challenges and limitations, such as low sensibility and detection limits, spectral interferences, homogeneity of the sample, sample preparation, calibration and normalization of the spatial resolution

limitations, and sample interactions with the electron beam. Table 1 shows the average composition obtained for the samples shown in Figure 3.

Table 1. Results of the analysis performed using SEM-EDS, showing the average semi-quantitative and punctual composition results.

Element (% wt.)	IJ	IJ-D	IJ-As	IJ-Cr	IJ-As + Cr
O	46.42	47.83	46.87	47.32	45.76
Fe	25.47	31.25	26.58	27.85	27.52
S	12.12	4.58	12.39	11.39	10.62
Na	3.79	1.39	3.88	5.23	4.25
Al	0.98	0.86	0.84	1.17	2.35
Zn	3.12	11.34	2.45	3.96	1.89
Si	1.02	1.09	1.59	1.22	3.94
K	1.16	1.01	---	0.29	---
As	0.44	---	1.01	---	1.04
Cr	---	---	---	0.08	0.28
Cu	1.78	0.65	1.54	1.49	2.35
Pb	3.69	---	2.85	---	---

From the results observed in Table 1, it can be seen that the IJ initially contains As (0.44%), which originates from the minerals treated in the early stages of concentration and that may have been part of arsenopyrite or arsenocopper pyrite, among others. In the case of decomposed IJ, it is observed that the contents of S, Na, and Cu decrease, while Pb and As no longer appear, which is the result of the dissolution of sulfate and associated metals, leaving a residue consisting of FeOH and franklinite, as seen in the DRX results. Finally, for the solids IJ-As, IJ-Cr, and IJ-As + Cr, the presence of As (1.01%), Cr (0.08), and As + Cr (1.04 and 0.28%) can be observed. This confirms the ability of this residue to desorb and re-adsorb As and, additionally, Cr.

It is important to mention that during the adsorption process, jarosite is formed by amorphous iron hydroxides with a rather porous morphology. It also contains elements such as Si, Zn, Cu, and Al, which can form complexes with both As and Cr, promoting, to a certain extent, the adsorption of these heavy metals, or forming reactive species with iron (Al, Zn, and Si), which can be more reactive toward As(V) and Cr(III). Likewise, Cu can act as a catalyst and, at some point, oxidize Cr(III) into Cr(VI), which can affect the adsorption of this element. However, Cu can also form complexes with As(V), and this would lead to an increase in the adsorption of As. Finally, it is important to highlight that the influence of each and every one of these elements on the adsorption of As(V) and Cr(III) will depend on various factors, such as the concentration of each element, the pH value of the solution, temperature, and the presence of other ions [65].

3.3. FTIR Analysis

An FTIR analysis for inorganic materials provides information on the molecular structure and chemical composition of the material. This analysis can provide information to identify functional groups and study the molecular interactions, among other determinations [66].

For the present study, Figure 4 shows the spectra obtained by FTIR for IJ, decomposed IJ, IJ with As, IJ with Cr, and IJ with As + Cr particles.

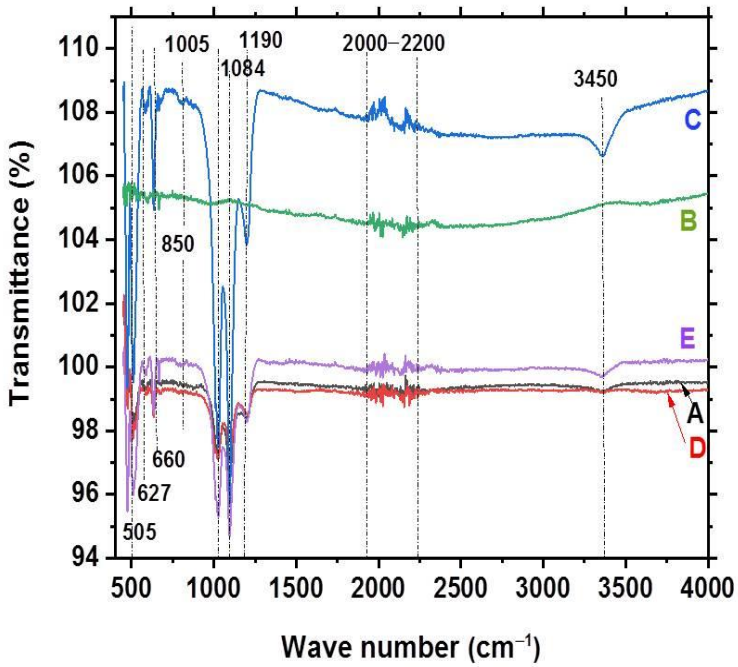

Figure 4. FTIR spectra obtained for (A) IJ; (B) decomposed IJ; (C) IJ with As adsorbed; (D) IJ with Cr adsorbed, and (E) IJ with As-Cr adsorbed.

In the FTIR spectrum observed in Figure 4, the results obtained for the samples of industrial jarosite (A), decomposed industrial jarosite (B), industrial jarosite with adsorbed As (C), industrial jarosite with adsorbed Cr (D), and industrial jarosite with adsorbed As + Cr (E) are shown. In the case of spectra A, C, D, and E, absorption bands in the 3400–3700 cm^{-1} region are observed, which correspond to the OH^- groups of the jarosite. Similarly, adsorption bands in the 1000–1200 cm^{-1} region (1005, 1084, and 1190 cm^{-1}) are observed, which correspond to regions representing the stretching vibration of the sulfate (SO_4^{-2}) groups. Absorption bands in the 500–700 cm^{-1} region are also observed, which represent the stretching vibration of the Fe-O bonds. Finally, to fully confirm the existence of jarosite in each sample, the 400–500 cm^{-1} region is examined, which reflect the absorption bands due to the bending vibration of the hydroxyl (OH^-) groups.

For the case of As(V), in spectra C and E, small absorption bands are observed in the 850–950 cm^{-1} region, where the As-O stretching vibration is located. Additionally, absorption bands can be observed in the 500–600 cm^{-1} region, which correspond to the bending vibration of the As-O bond. Similarly, arsenate can be localized in the absorption region corresponding to 870–920 cm^{-1}, which is attributed to the As-O stretching vibration of the arsenate group [56,67]. Likewise, the presence of bonds in the 2050–2150 cm^{-1} region, which may correspond to the As=O, As-O, Cr=O, and Cr-O bonds [56].

On the other hand, the identification of Cr(III) in spectra D and E can be obtained by finding the most common absorption bands. These can be found in the 600–700 cm^{-1} region, attributed to the Cr-O stretching vibration, while for the Cr-O bending vibration, they can be found in the 400–500 cm^{-1} region. However, it should be taken into account that the exact positions of each absorption band can vary depending on the chemical form of both As and Cr, as well as on the presence of other ions or molecules in the sample.

Finally, spectrum B shows practically no observable absorption bands, since the crystalline structure of the compounds was destroyed and few bonds remained, and those that did were too weak at the end of said decomposition.

3.4. XPS Analysis

This analysis helps to determine elemental composition, identifying the elements present in a sample, its chemical state (oxidation state and chemical bonding), surface chemistry, and binding energies of the electrons of the atoms composing the sample [68]. Overall, XPS provides valuable information on the surface and bulk composition, chemical state, and bonding of inorganic materials.

Figure 5 shows the XPS spectra for the IJ (Figure 5A) and decomposed IJ (Figure 5B).

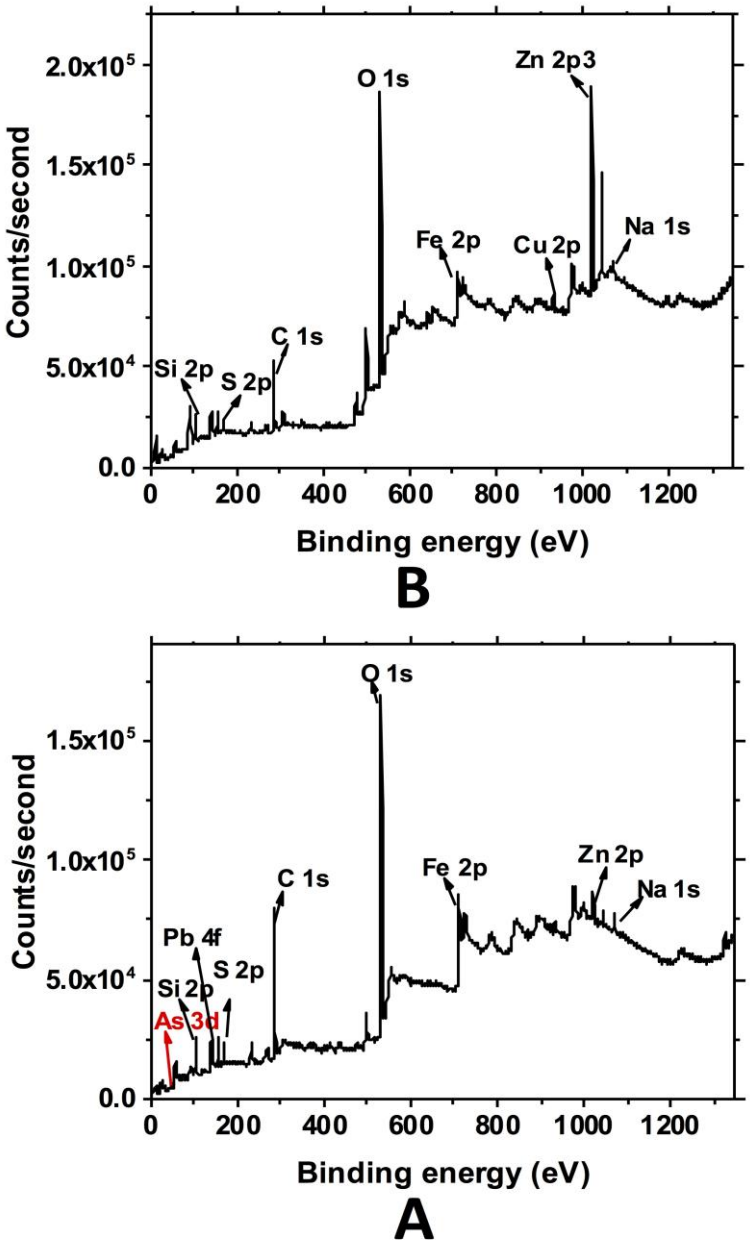

Figure 5. XPS spectra obtained for (**A**) IJ and (**B**) decomposed IJ.

In Figure 5A, the presence of O, S, Fe, Na, and Pb is observed, which form part of the chemical composition of jarosite. Similarly, the presence of Zn is noted, which is part of the franklinite found in DRX, and the presence of As is again noted (0.67% in this case), which, as mentioned earlier, comes from minerals associated with sphalerite, such as arsenopyrite, and which were leached and incorporated into the jarosite structure during its precipitation in the leaching circuits.

On the other hand, spectrum B no longer shows the presence of As and Pb, and the counts per second for S and Na have decreased, which did not happen for Fe and Zn. This confirms the decomposition of the industrial jarosite.

For the case of the XPS results obtained for the IJ with As, IJ with Cr, and IJ with As+Cr, Figure 6 shows these spectra, demonstrating the incorporation of As and Cr into the jarosite structure and also showing the presence of the elements found in spectra 5A.

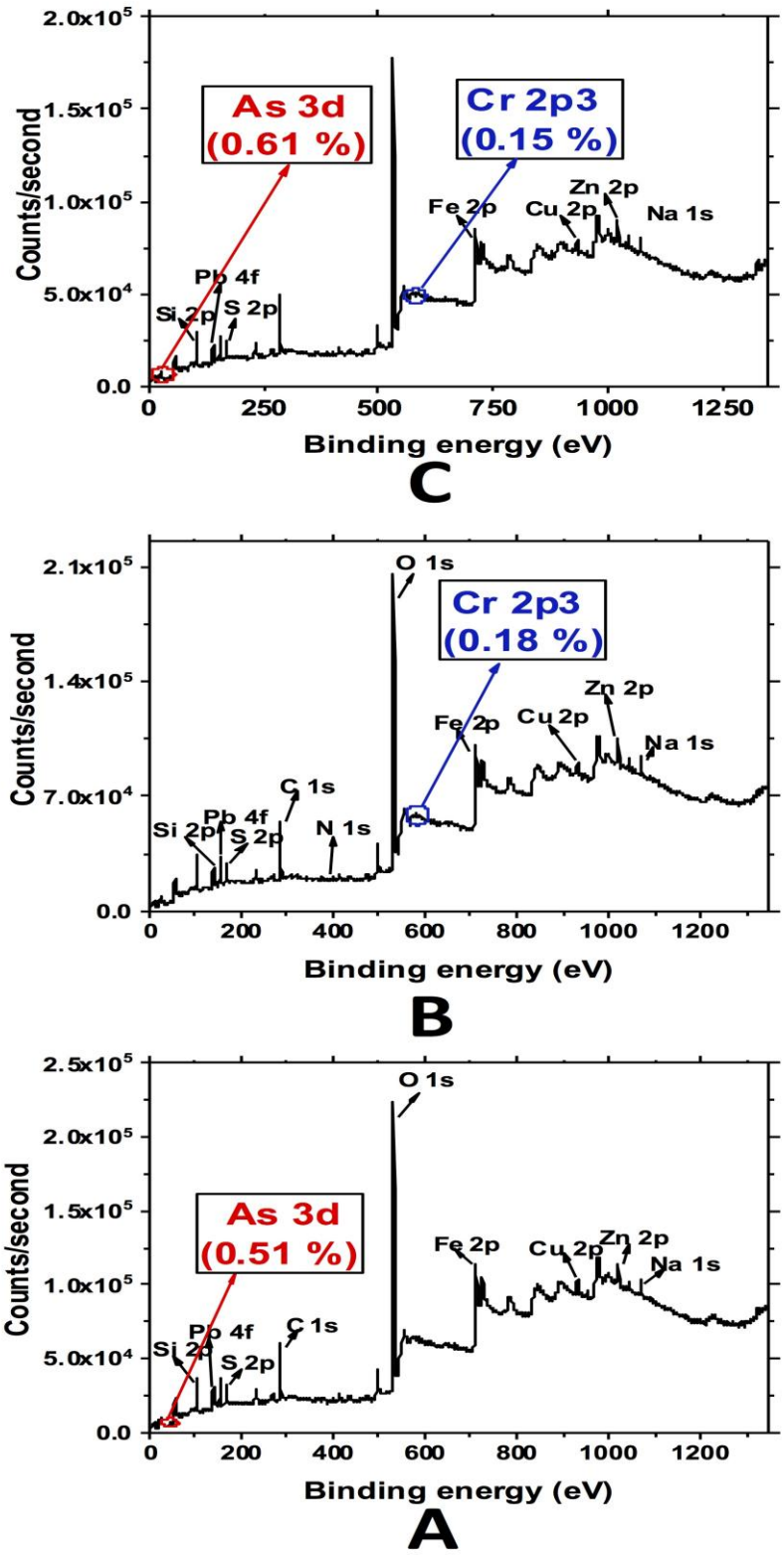

Figure 6. XPS spectra obtained for (**A**) IJ with As, (**B**) IJ with Cr, and (**C**) IJ with As+Cr.

3.5. ICP Analysis

The ICP analysis provides information on the elemental composition of a sample. The results of an ICP analysis can include elemental concentrations, elemental identifications, isotropic ratios, contaminant detection, and elemental speciation [69].

Based on the results obtained, adsorption of 90.6% of As(V) and 96.3% of Cr(III) was achieved from synthetic solutions with known contents of each metal, after a process carried out for 60 min at room temperature. Similarly, for the evaluation of the joint adsorption of As(V) and Cr(III), the percentages obtained were 57% for As(V) and 75.1% for Cr(III).

A discrepancy was noted in the adsorbed contents of As(V) and Cr(III) when the adsorption of each metal was evaluated individually versus simultaneously. In both scenarios, a higher percentage of Cr adsorption was observed compared with As, which is potentially attributed to the presence of Cu in the jarosite, which may have oxidized Cr(III) to Cr(VI), thereby enhancing its adsorption. Additionally, the presence of Zn, Al, and Si may have facilitated the formation of more reactive species with the Fe ions [65].

The adsorption efficiency of 90.6% for As(V) and 96.3% for Cr(III) obtained in this study is remarkably high compared with that in previous studies that have used different adsorbent materials (natural and synthesized) [13,16,20,70]. For example, previous studies have reported adsorption efficiencies for As(V) ranging from 40% to 80% using materials such as iron oxides, clays, and activated carbons [15,25,71–73]. The high adsorption efficiency observed in the present study can be attributed to the presence of functional groups on the surface of the industrial jarosite that can interact with As(V) and Cr(III) ions. More specifically, the adsorption of these ions on the decomposed jarosite particles, which are mainly composed of iron hydroxide with high porosity, may be due to adsorption on the surface due to electrostatic and Van der Waals interactions between the ions and the surface. An exchange of As and Cr ions with Fe ions on the surface of the material may also occur, which may be favored by the formation of reactive species that are formed with elements such as Zn, Al, and Si, or by the presence of Cu, which manages to oxidize Cr and thus favor the adsorption of this element. Likewise, precipitation of the ions on the surface of the material and diffusion toward the matrix through the pores of the material may occur.

Additionally, the decomposition of industrial jarosite at alkaline pH may have released iron ions and other metals that may have contributed to the adsorption of As(V) and Cr(III) ions [21,74,75].

These results are preliminary and require further in-depth studies. However, there appears to be competition between As(V) and Cr(III) when both ions are present simultaneously, and Cr apparently wins the location on the decomposed IJ when As is present. Nevertheless, the adsorption of Cr(III) appears to be more efficient than of As(V), which, as was discussed, could be due to the presence of elements such as Zn, Al, Si, and Cu in the decomposed jarosite. And despite everything, the efficiency of heavy metal adsorption using mining waste is a reality.

Future studies should investigate the ability of industrial jarosite to adsorb other ions and contaminants, such as heavy metals and radionuclides. Additionally, it would be beneficial to study the stability and durability of industrial jarosite under different environmental conditions and uses. Finally, it is important to evaluate the economic and environmental viability of industrial jarosite as an adsorbent material compared with other materials available on the market.

4. Conclusions

Industrial jarosite has proven to be a highly effective adsorbent material for the removal of As(V) and Cr(III) from aqueous solutions, achieving adsorption efficiencies of 90.6% and 96.3%, respectively, under the experimental conditions evaluated in this research

study. The adsorption process is attributed to the presence of functional groups on the surface of the material that interact with metal ions, and the recrystallization of industrial jarosite after adsorption suggests that the material undergoes structural and chemical changes during the process. Giving its effectiveness and potential cost-effectiveness, industrial jarosite may offer a viable solution for the remediation of soils and waters contaminated with As(V) and Cr(III), providing a more affordable alternative to other materials. However, further studies are necessary to evaluate the stability and durability of industrial jarosite under various environmental conditions and uses, as well as to explore its potential for the adsorption of other contaminants, ultimately unlocking its full potential for environmental remediation applications.

Author Contributions: Conceptualization, E.S.-R., M.C.-H., A.G.-C. and R.G.S.M.; methodology, E.S.-R., J.H.-Á. and F.R.B.-H.; software, N.T., M.S. and M.P.G.-A.; validation, J.F.-B., E.C.-S., I.A.C.-E. and E.S.-R.; formal analysis, M.C.-H., A.G.-C. and R.G.S.M.; investigation, E.S.-R., and J.H.-Á.; resources, E.S.-R., J.H.-Á., and N.T.; data curation, M.S., M.P.G.-A. and M.C.-H.; writing—original draft preparation, E.S.-R. and F.R.B.-H.; writing—review and editing, M.C.-H., A.G.-C., R.G.S.M. and I.A.C.-E.; visualization, F.R.B.-H. and E.S.-R.; supervision, E.S.-R. and F.R.B.-H.; project administration, E.S.-R. and J.H.-Á.; funding acquisition, E.S.-R. and F.R.B.-H. All authors have read and agreed to the published version of the manuscript.

Funding: This research received no external funding.

Institutional Review Board Statement: Not applicable.

Informed Consent Statement: Not applicable.

Data Availability Statement: The original contributions presented in the study are included in the article; further inquiries can be directed to the corresponding authors.

Acknowledgments: The authors would like to acknowledge the support providen by the Academic Area of Earth Sciences and Materials of the UAEH. They also gratefully acknowledge CONAHCyT for the scholarships granted to the student M.C.-H. (774130, and CVU 1076684) and I.A.C.-E. (CVU 502633).Additionally, M.S. acknowledges the infrastructure and support from "Doctorado en Ingeniería de Procesos de Minerales" at the Universidad de Antofagasta. Finally, the authors acknowledge the suppot provided by Edelmira Gálvez from the Universidad Católica del Norte, Chile.

Conflicts of Interest: The authors declare no conflicts of interest.

References

1. Barbier, E.B.; Burgess, J.C. Economics of Water Scarcity and Efficiency. *Sustainability* **2024**, *16*, 8550. [CrossRef]
2. Pontius, J.; Mclntosh, A. Chapter: Water Scarcity. In *Environmental Problem Solving in an Age of Climate Change, Voleme One: Basic Tools and Techniques*, 1st ed.; Sringer Nature: New York, NY, USA, 2024; pp. 81–103. [CrossRef]
3. Tzanakakis, V.A.; Paranychianakis, N.V.; Angelakis, A.N. Water Supply and Water Scarcity. *Water* **2020**, *12*, 2347. [CrossRef]
4. Pierrat, É.; Laurent, A.; Dorber, M.; Rygaard, M.; Verones, F.; Hauschild, M. Advancing water footprint assessments: Combining the impacts of water pollution and scarcity. *Sci. Total Environ.* **2023**, *870*, 161910. [CrossRef]
5. Han, L.; Zhai, Y.; Chen, R.; Fan, Y.; Liu, Z.; Zhao, Y.; Li, R.; Xia, L. Characteristics of Soil Arsenic Contamination and the Potential of Pioneer Plants for Arsenic Remediation in Gold Mine Tailings. *Toxics* **2023**, *11*, 1025. [CrossRef] [PubMed]
6. Endara, A.D.L.M.G.; Heinert, M.E.; Solórzano, H.X.P. Contaminación del agua y aire por agentes químicos. *Recimundo* **2020**, *4*, 79–93. (In Spanish) [CrossRef]
7. Singh, J.; Yadav, P.; Pal, A.K.; Mishra, V. Water Pollutants: Origin and Status. In *Sensors in Water Pollutants Monitoring: Role of Materials*, 1st ed.; Pooja, D., Kumar, P., Singh, P., Patil, S., Eds.; Springer: New York, NY, USA, 2020; Volume 1, pp. 5–20. [CrossRef]
8. Madhav, S.; Ahamad, A.; Singh, A.K.; Kushawaha, J.; Chauhan, J.S.; Sharma, S.; Singh, P. Water Pollutants: Sources and Impact on the Environment and Human Health. In *Sensors in Water Pollutants Monitoring: Role of Materials*, 1st ed.; Pooja, D., Kumar, P., Singh, P., Patil, S., Eds.; Springer: New York, NY, USA, 2020; Volume 1, pp. 43–62. [CrossRef]
9. Nti, E.K.; Cobbina, S.J.; Attafuah, E.E.; Senanu, L.D.; Amenyeku, G.; Gyan, M.A.; Forson, D.; Safo, A. Water pollution control and revitalization using advanced technologies: Uncovering artificial intelligence options towards environmental health protection, sustainability and water security. *Heliyon* **2023**, *9*, e18170. [CrossRef] [PubMed]

10. Rashid, A.; Schutte, B.J.; Ulery, A.; Deyholos, M.K.; Sanogo, S.; Lehnhoff, E.A.; Beck, L. Heavy Metal Contamination in Agricultural Soil: Environmental Pollutants Affecting Crop Health. *Agronomy* **2023**, *13*, 1521. [CrossRef]
11. Zhang, P.; Yang, M.; Lan, J.; Huang, Y.; Zhang, J.; Huang, S.; Yang, Y.; Ru, J. Water Quality Degradation Due to Heavy Metal Contamination: Health Impacts and Eco-Friendly Approaches for Heave Metal Remediation. *Toxics* **2023**, *11*, 828. [CrossRef]
12. Tan, H.W.; Pang, Y.L.; Lim, S.; Chong, W.C. A state-of-the-art of phytoremediation approach for sustainable management of heavy metals recovery. *Environ. Technol. Innov.* **2023**, *30*, 103043. [CrossRef]
13. López-Martínez, A.M.; Gamero-Melo, P. Mild Conditions Method to Remediate Hazardous Jarosite and Its Application as Adsorbent of Arsenic (V) and Water. *Minerals* **2023**, *13*, 1148. [CrossRef]
14. Cerecedo-Sáenz, E.; Hernández-Lazcano, E.; Gonzalez-Bedolla, M.J.; Hernández-Ávila, J.; Roisales-Ibáñez, R.; Gutiérrez-Amador, M.P.; Sánchez-Castillo, A.; Arenas-Flores, A.; Salinas-Rodríguez, E. Synthesis, Characterization and Decomposition of Potassium Jarosite for Adsorptive As(V) Removal in Contaminated Water: Preliminary Study. *Int. J. Environ. Res. Public. Health* **2022**, *19*, 15912. [CrossRef] [PubMed]
15. Liu, J.B.; Zhang, H.; Wang, H.; He, B.; Wang, H.; Jin, R.; Tian, T. Remediation of arsenic-and nitrate-contaminated groundwater through iron-dependent autotrophic denitrifying culture. *Environ. Res.* **2024**, *257*, 119239. [CrossRef] [PubMed]
16. Kumar, A.; Bhattacharya, T.; Shaikh, W.A.; Biswas, J.K. Valorization of invasive plant and leaf litter wastes into biochar: Production, properties and potential for arsenic removal. *Groundw. Sustain. Dev.* **2024**, *24*, 101066. [CrossRef]
17. Wei, M.; Wang, B.; Wu, P.; Zhang, X.; Chen, M.; Wang, S. Electrolytic manganese residue-biochar composite for simultaneous removal of antimony and arsenic from water: Adsorption performance and mechanisms. *J. Clean. Prod.* **2024**, *437*, 140623. [CrossRef]
18. Wang, L.K.; Wang, M.H.S.; Shammas, N.K.; Hahn, H.H. Physicochemical Treatment Consisting of Chemical Coagulation, Precipitation, Sedimentation, and Flotation. In *Integrated Natural Resources Research. Handbook of Environmental Engineering*, 1st ed.; Wang, L.K., Wang, M.H.S., Hung, Y.T., Eds.; Springer: New York, NY, USA, 2021; Volume 22, pp. 265–397. [CrossRef]
19. Li, J.; Tao, L.; Sun, W.; Lu, Z.; Li, J.; Qiu, S. Arsenic removal from coal by ferric chloride enhanced leaching under ultraviolet irradiation during flue gas desulphuration with coal slurry. *Environ. Technol.* **2023**, *45*, 5004–5015. [CrossRef]
20. Elgarhy, G.S.; El-Subruiti, G.M.; Omer, A.M.; Eltaweil, A.S. 2D/3D MXene/NiFeMn-layered double hydroxide decorated gelatin for removal of Cr(VI) and Congo red: Performance and mechanism. *J. Mol. Liq.* **2024**, *396*, 123889. [CrossRef]
21. Ortíz-Quiñonez, J.L.; Cancino-Gordillo, F.E.; Pal, U. Removal of Cr(III) Ions from Water Using Magnetically Separable Graphene-Oxide-Decorated Nickel Ferrite Nanoparticles. *ACS Appl. Nano Mater.* **2023**, *6*, 18491–18507. [CrossRef]
22. Vasylyeva, H.; Mironyuk, I.; Strilchuk, M.; Maliuk, I.; Savka, K.; Vasyliev, O. Adsorption and possibility of separation of heavy metal cations by strong cation exchange resin. *Chem. Phys. Impacts* **2021**, *3*, 100056. [CrossRef]
23. Ahmer, M.F.; Uddin, M.K. Structure properties and industrial applications of anion exchange resins for the removal of electroactive nitrate ions from contaminated water. *RSC Adv.* **2024**, *14*, 33629–33648. [CrossRef] [PubMed]
24. Adam, M.R.; Othman, M.H.D.; Kurniawan, T.A.; Puteh, M.H.; Ismail, A.F.; Khongnakorn, W.; Rahman, M.A.; Jaafar, J. Advances in adsortive membrane technology for water treatment and resource recovery applications: A critical review. *J. Environ. Chem. Eng.* **2022**, *10*, 107633. [CrossRef]
25. Kinoti, I.K.; Ogunah, J.; M'Thiruaine, C.M.; Marangu, J.M. Adsorption of Heavy Metals in Contaminated Water Using Zeolite Derived from Agro-Wastes and Clays: A Review. *J. Chem.* **2022**, *2022*, 4250299. [CrossRef]
26. Chen, X.C.; Huang, Z.J.; Wuang, A.; Yu, J.Y.; Zhang, J.Y.; Xiao, Z.J.; Cui, X.Y.; Liu, X.H.; Yin, N.Y.; Cui, Y.S. Immobilisation remediation of arsenic-contaminated soils with promising CaAl-layered double hydroxide and bioavailability, bioaccessibility, and speciation-based health risk assessment. *J. Hazard. Mater.* **2024**, *469*, 134096. [CrossRef]
27. Ai, J.; Abdelraheem, W.H.M.; Peng, S.; Zhang, W.; Wang, Q.; Dionysiou, D.D. As^{III}-enhanced oxidation by coexisting Mn^{III}-phenolic complexes during arsenic contaminated groundwater treatment by MnO_2. *Sep. Purif. Technol.* **2024**, *344*, 127254. [CrossRef]
28. Yang, Y.; Wang, Y.; Xue, C.; Lin, Y.; Lee, J.F.; Yi, X.; Dang, Z. Efficient removal of heavy metals from acid mine drainage by ε-MnO_2 adsorption. *J. Clean. Prod.* **2024**, *452*, 141936. [CrossRef]
29. Shi, L.; Zhu, Z.; Wu, N.; Chang, Y.; Yue, L.; An, L. Natural hydroxyapatite powder from pig-bone waste (pHAP) for the rapid adsorption of heavy metals (Cu) in aqueous solution. *Adsorption* **2024**, *30*, 801–812. [CrossRef]
30. Rafiq, K.; Sultana, M.; Abid, M.Z.; Quyyum, U.; AlMasoud, N.; Alomar, T.S.; El-Bahy, A.M.; Nasir, M.H.; Hussain, E. Unveiling the impact and selectivity of $BiVO_4$/rGO-SiO_2 adsorbents for arsenic in ground water: An effective approach for the public safety. *J. Ind. Eng. Chem.* **2024**, *139*, 336–346. [CrossRef]
31. Kotnala, S.; Bhushan, B.; Nayak, A. Hydroxyapatite@cellulose@nZVI composite: Fabrication and adsorptive removal of doxycycline, Cr(VI) and As(III) from wastewater. *Chem. Eng. Sci.* **2024**, *288*, 119796. [CrossRef]
32. Scheverin, V.N.; Diaz, E.M.; Horst, M.F.; Lassalle, V.L. Synthesis of novel magnetic hydroxyapatite-biomass nanocomposite for arsenic and fluoride adsorption. *Environ. Geochem. Health* **2024**, *46*, 190. [CrossRef]

33. Li, Y.; Wang, J.; Liu, C.; Wang, L.; Zhang, P.; Zhao, Q.; Xiong, Z.; Zhang, G.; Zhang, W. Remediation of arsenic-contaminated soil using nanoscale schwertmannite synthesized by persulfate oxidation with carboxymethyl cellulose stabilization. *Environ. Res.* **2024**, *244*, 117931. [CrossRef] [PubMed]
34. Wang, X.; Wang, L.; Fu, J.; Zhang, Y.; Dong, Y.; Zheng, G.; Zhou, L. Enhancing Coimmobilisation Capacity of Schwertmannite for Arsenic and Cadmium through pH Elevation after Chemical Oxidation. *ACS ES&T Eng.* **2024**, *4*, 409–418. [CrossRef]
35. Tu, Y.; Fan, X.; Zhao, Y.; Wu, C.; Liu, Y.; Wu, W.; Zhao, D. Sulfidation of nano-Fe/Pd bimetal for highly efficient remediation of Cr(VI) from water: Enhanced reactivity and applicability. *Inor. Chem. Commun.* **2024**, *162*, 112278. [CrossRef]
36. Wang, C.; Chen, K.; Yin, M.; Zhou, Y.; Zhuang, Q.; Cao, Q.; Dang, Z.; Guo, C. Surface properties of schwertmannite with different sulfate contents and its effect on Cr(VI) adsorption. *Geochim. Cosmochim. Acta* **2024**, *373*, 245–258. [CrossRef]
37. Fernandez-Rojo, L.; Marti, V.; Jubany, I.; Bahí, N.; Janer, M.; Martínez-Lladó, X.; Rovira, M. Improvement in Arsenic Adsorption and Calcite Dissolution Kinetics through Size Reduction of a Ferric Hydroxyde-Calcite Adsorbent. *Water* **2023**, *16*, 30. [CrossRef]
38. Avola, T.; Campisi, S.; Polito, L.; Arici, S.; Ferruti, L.; Gervasini, A. Adressing the issue of surface mechanisms and competitive effects in Cr (VI) reductive-adsorption on tin-hydroxyapatite in the presence of co-ions. *Sci. Rep.* **2023**, *13*, 18913. [CrossRef] [PubMed]
39. Joya-Cárdenas, D.R.; Rodríguez-Caicedo, J.P.; Corona-Rivera, M.A.; Saldaña-Robles, N.; Damián-Ascencio, C.E.; Saldaña-Robles, A. Removal of As(V) in the presence of Cr(VI) in contaminated water from the Bajio region of Mexico using ferrihydrite-functionalized graphene oxide (GOFH): A case study. *Emerg. Contam.* **2024**, *10*, 100312. [CrossRef]
40. Hudson-Edwards, K.A. Uptake and release of arsenic and antimony in alunite-jarosite and beudantite group minerals. *Am. Mineral.* **2019**, *104*, 633–640. [CrossRef]
41. Bari, A.F.; Choppola, G.; Lamb, D.; Hamilton, J.L.; Sathish, C.I.; Rahman, M.M.; Naudi, R.; Aughterson, R.; Burton, E.D. Is beudantite a stable host phase of arsenic and lead? New insights from molecular-scale kinetic analysis. *J. Hazard. Mater.* **2024**, *480*, 136382. [CrossRef]
42. Tang, Z.; Tang, X.; Xiao, Z.; Liu, H. Mechanism and thermodynamics of scorodite formation by oxidative precipitation from arsenic-bearing solution. *Environ. Res.* **2024**, *250*, 118500. [CrossRef]
43. Su, R.; Su, X.; Gao, Y.; Ma, X.; Zhao, X.; Ou, X.; Cui, Y.; Lin, J.; Pan, Y.; Wang, S. Cotreatment strategy for hazardous arsenic-calcium residue and siderite tailings via arsenic fixation as scorodite. *J. Environ. Sci.* **2024**, *153*, 118–127. [CrossRef]
44. Viñals, J.; Sunyer, A.; Molera, P.; Cruells, M.; Llorca, N. Arsenic stabilization of calcium arsenate waste by hydrothermal precipitation of arsenical natroalunite. *Hydrometallurgy* **2010**, *104*, 247–259. [CrossRef]
45. Sunyer, A.; Viñals, J. Arsenate substitution in natroalunite. A potential medium for arsenic immobilization. Part 1. Synthesis and compositions. *Hydrometallurgy* **2011**, *109*, 54–64. [CrossRef]
46. Sunyer, A.; Viñals, J. Arsenate substitution in natroalunite. A potential medium for arsenic immobilization. Part 2. Cell parameters and stability tests. *Hydrometallurgy* **2011**, *109*, 106–115. [CrossRef]
47. Zhang, Y.; Deng, Y.; Xue, J.; Cheng, Y.; Nie, Y.; Pi, K.; Du, Y.; Xie, X.; Shi, J.; Wuang, Y. Unravelling the impacts of soluble Mn(II)-NOM on arsenic immobilization by ferrihydrite or goethite under aquifer conditions. *J. Hazard. Mater.* **2024**, *466*, 133640. [CrossRef] [PubMed]
48. Chen, K.; Guo, C.; Wuang, C.; Zhao, S.; Xiong, B.; Lu, G.; Reinfelder, J.R.; Dang, Z. Prediction of Cr(VI) and As(V) adsorption on goethite using hybrid surface complexation-machine learning model. *Water Res.* **2024**, *256*, 121580. [CrossRef] [PubMed]
49. Nolasco, M.C.; Flores, L.F.; Gutiérrez, E.J.; Aguilar, J.; Palacios, E.G.; Flores, M.U.; Rodríguez, I.; Reyes, I.A. Acid dissolution of jarosite-type compounds: Effect of the incorporation of divalent cations into the structure on the reaction rate. *Hydrometallurgy* **2022**, *212*, 105907. [CrossRef]
50. Picazo-Rodríguez, N.G.; Soria-Aguilar, M.D.J.; Chaidez, J.; Flores, M.; Almaguer-Guzmán, I.; Carrillo-Pedroza, F.R. Analysis of the Behavior of As and Pb during the Pretreatments Applied to a Jarosite Residue for the Recovery of Gold and Silver. *Metals* **2023**, *13*, 138. [CrossRef]
51. López-Martínez, A.M.; Khamkure, S.; Gamero-Melo, P. Bifunctional Adsorbents Based on Jarosites for Removal of Inorganic Micropollutants from Water. *Separations* **2023**, *10*, 309. [CrossRef]
52. Sowers, T.D.; Blackmon, M.D.; Betts, A.R.; Jerden, M.L.; Scheckel, K.G.; Bradham, K.D. Potassium jarosite seeding of soils decreases lead and arsenic bioaccessibility: A path toward concominant remediation. *Proc. Natl. Acad. Sci. USA* **2023**, *120*, e2311564120. [CrossRef]
53. Guo, J.; Zhou, Z.; Yuan, J.; Liu, C.; Ke, P.; Zhao, B.; Hu, Z. Effect of preparation methods on the morphology of jarosite and its adsorption performance for U(VI). *J. Ranioanal Nucl. Chem.* **2024**, *333*, 317–328. [CrossRef]
54. Jin, X.; Guo, C.; Huang, Q.; Tao, X.; Li, X.; Xie, Y.; Dang, Z.; Zhou, J.; Lu, G. Arsenic redistribution associated with Fe(II)-induced jarosite transformation in the presence of polygalacturonic acid. *Sci. Total. Environ.* **2024**, *935*, 173444. [CrossRef]
55. Jhariya, U.; Chien, M.F.; Umetsu, M.; Kamitakahara, M. Effective selenate removal using pH modulated synthesis of biogenic jarosite: Comparative insight with non-biogenic jarosite and biogenic schwertmannite. *J. Hazard. Mater.* **2024**, *480*, 136256. [CrossRef] [PubMed]

56. Smith, B.C. *Fundamentals of Fourier Transform Infrared Spectroscopy*, 2nd ed.; CRC Press: Boca Raton, FL, USA, 2020; pp. 1–175.
57. Gong, Y.; Chen, X.; Wu, W. Application of fourier transform infrared (FTIR) spectroscopy in sample preparation: Material characterization and mechanism investigation. *Adv. Sample Prep.* **2024**, *11*, 100122. [CrossRef]
58. Silverstein, R.M.; Bassier, C. Spectrometric identification of organic compounds. *J. Chem. Educ.* **1962**, *39*, 546. [CrossRef]
59. Chen, Y.; Zou, C.; Mastalerz, M.; Hu, S.; Gasaway, C.; Tao, X. Applications of Micro-Fourier Transform Infrared Spectroscopy (FTIR) in the Geological Sciences—A Review. *Int. J. Mol. Sci.* **2015**, *16*, 30223–30250. [CrossRef]
60. Cruells, M.; Roca, A. Jarosites: Formation, Structure, Reactivity and Environmental. *Metals* **2022**, *12*, 802. [CrossRef]
61. Salinas, E.; Roca, A.; Cruells, M.; Patiño, C.; Córdoba, D.A. Characterization and alkaline decomposition-cyanidation kinetics of industrial ammonium jarosite in NaOH media. *Hydrometallurgy* **2001**, *60*, 237–246. [CrossRef]
62. Feng, X.; Long, R.; Wang, L.; Liu, C.; Bai, Z.; Liu, X. A review on heavy metal ions adsorption from water by layered double hydroxide and its composites. *Sep. Purif. Technol.* **2022**, *284*, 1200999. [CrossRef]
63. Biedunkova, O.; Kuznietsov, P.; Gandziura, V. Behaviour of dissolved inorganic salts in the cooling water of a nuclear power plant open recirculation system and formation of water discharge. *R. Soc. Open. Sci.* **2024**, *11*, 240492. [CrossRef] [PubMed]
64. Li, K.J.; Kurniawan, A.; Christidis, G.E.; He, J.Y.; Zhuo, C.H. Interfacial interactions controlling adsorption of metal cations on montmorillonite. *Am. Min.* **2024**, *109*, 633–655. [CrossRef]
65. Esfandiar, N.; Suri, R.; McKenzie, E.R. Competitive sorption of Cd, Cr, Cu, Ni, Pb and Zn from stormwater runoff by five low-cost sorbents; Effects of co-contaminants, humic acid, salinity and pH. *J. Hazard. Mater.* **2022**, *423*, 126938. [CrossRef] [PubMed]
66. Larkin, P. *Infrared and Raman Spectroscopy: Principles and Spectral Interpretation*, 2nd ed.; Elsevier: Amsterdam, The Netherlands, 2017; pp. 1–276. ISBN 978-0-12-804162-8.
67. Bullen, J.C.; Lapinee, C.; Miller, L.A.; Bullough, F.; Berry, A.J.; Najorka, J.; Cibin, G.; Vilar, R.; Weiss, D.J. Spectroscopic (XAS, FTIR) investigations into arsenic adsorption onto TiO_2/Fe_2O_3 composites: Evaluation of the surface complexes, speciation and precipitation predicted by modelling. *Results Surf. Interfaces* **2022**, *9*, 100084. [CrossRef]
68. Van der Heide, P. *X-ray Photoelectron Spectroscopy: An Introduction to Principles and Practices*, 1st ed.; John Willey & Sons: Hoboke, NJ, USA, 2011; pp. 1–256. ISBN 978-1-118-06253-1.
69. Ali, I.; Aboul-Enein, H.Y. *Instrumental Methods in Metal Ion Speciation*, 1st ed.; CRC Press: Boca Raton, FL, USA, 2006; pp. 1–376. [CrossRef]
70. Rafiq, K.; Asghar, S.; Abid, M.Z.; Sultana, M.; Waleed, M.Z.; Hashem, A.; Avila-Quezada, G.D.; Abd_Allah, E.F.; Hussain, E. Unveiling the potential of Fe_2O_3/TiO_2 system to produce clean water: An effective and low-cost approach for arsenic removal from ground water. *Surf. Interfaces* **2024**, *52*, 104913. [CrossRef]
71. Liang, Y.; Tang, L.; Jiang, J.; Li, M.L.; Lv, H.G.; He, Y.; Liu, H.Y.; Xue, S.G. Dual-supported nanoscale zero-valent iron for As(III) contaminated groundwater remediation. *J. Environ. Chem. Eng.* **2023**, *11*, 111111. [CrossRef]
72. Chi, Z.; Xie, X.; Pi, K.; Wu, Y.; Wang, Y. Spectroscopic and modeling approaches of arsenic (III/V) adsorption onto Illite. *J. Hazard. Mater.* **2024**, *447*, 135284. [CrossRef]
73. Singh, R.; Singh, S.; Parihar, P.; Singh, V.P.; Prasad, S.M. Arsenic contamination, consequences and remediation techniques: A review. *Ecotoxicol. Environ. Saf.* **2015**, *112*, 247–270. [CrossRef]
74. Gareev, K.G. Diversity of Iron Oxides: Mechanisms of Formation, Physical Properties and Applications. *Magnetochemistry* **2023**, *9*, 119. [CrossRef]
75. Tripathy, J.; Mishra, A.; Pandey, M.; Thakur, R.R.; Chand, S.; Rout, P.R.; Shaid, M.K. Advances in Nanocomposites for Water and Wastewater Treatment: A Review. *Water* **2024**, *16*, 1481. [CrossRef]

Disclaimer/Publisher's Note: The statements, opinions and data contained in all publications are solely those of the individual author(s) and contributor(s) and not of MDPI and/or the editor(s). MDPI and/or the editor(s) disclaim responsibility for any injury to people or property resulting from any ideas, methods, instructions or products referred to in the content.